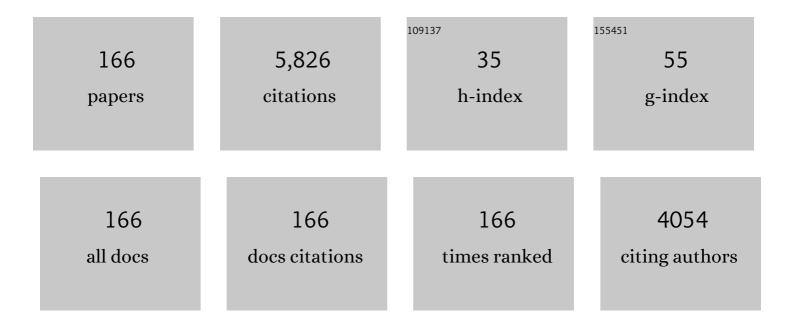
Jianhua Wang

List of Publications by Year in descending order

Source: https://exaly.com/author-pdf/1564164/publications.pdf Version: 2024-02-01



#	Article	IF	CITATIONS
1	Retinal microvascular density modifications during the water drinking test. European Journal of Ophthalmology, 2022, 32, 1602-1609.	0.7	1
2	Necroptosis in pulmonary macrophages promotes silica-induced inflammation and interstitial fibrosis in mice. Toxicology Letters, 2022, 355, 150-159.	0.4	6
3	Msi2â€mediated MiR7aâ€1 processing repression promotes myogenesis. Journal of Cachexia, Sarcopenia and Muscle, 2022, 13, 728-742.	2.9	18
4	Associations Between Lid Wiper Microvascular Responses, Lens Fit, and Comfort After One Day of Contact Lens Adaptation by Neophytes. Eye and Contact Lens, 2022, Publish Ahead of Print, .	0.8	0
5	The Effect of Software Versions on the Measurement of Retinal Vascular Densities Using Optical Coherence Tomography Angiography. Current Eye Research, 2021, 46, 341-349.	0.7	4
6	High resolution anterior segment optical coherence tomography of ocular surface lesions: a review and handbook. Expert Review of Ophthalmology, 2021, 16, 81-95.	0.3	2
7	Ocular surface microvascular response and its relation to contact lens fitting and ocular comfort: an update of recent research. Australasian journal of optometry, The, 2021, 104, 661-671.	0.6	1
8	Improvement of retinal tissue perfusion after circuit resistance training in healthy older adults. Experimental Gerontology, 2021, 146, 111210.	1.2	2
9	Longitudinal Study of Retinal Structure, Vascular, and Neuronal Function in Patients With Relapsing-Remitting Multiple Sclerosis: 1-Year Follow-Up. Translational Vision Science and Technology, 2021, 10, 6.	1.1	4
10	Effects of Ocufolin on retinal microvasculature in patients with mild non-proliferative diabetic retinopathy carrying polymorphisms of the MTHFR gene. BMJ Open Diabetes Research and Care, 2021, 9, e002327.	1.2	6
11	Retinal vessel density correlates with cognitive function in older adults. Experimental Gerontology, 2021, 152, 111433.	1.2	7
12	Discrimination of Diabetic Retinopathy From Optical Coherence Tomography Angiography Images Using Machine Learning Methods. IEEE Access, 2021, 9, 51689-51694.	2.6	14
13	RETINAL TISSUE PERFUSION REDUCTION BEST DISCRIMINATES EARLY STAGE DIABETIC RETINOPATHY IN PATIENTS WITH TYPE 2 DIABETES MELLITUS. Retina, 2021, 41, 546-554.	1.0	5
14	Retinal microvascular and neuronal function in patients with multiple sclerosis: 2-year follow-up. Multiple Sclerosis and Related Disorders, 2021, 56, 103314.	0.9	2
15	A suitable silicosis mouse model was constructed by repeated inhalation of silica dust via nose. Toxicology Letters, 2021, 353, 1-12.	0.4	12
16	Advances in ophthalmic structural and functional measures in multiple sclerosis: do the potential ocular biomarkers meet the unmet needs?. Current Opinion in Neurology, 2021, 34, 97-107.	1.8	2
17	Conjunctival Vessels in Diabetes Using Functional Slit Lamp Biomicroscopy. Cornea, 2021, 40, 950-957.	0.9	3
18	Retinal vessel density correlates with cognitive function in older adults. Alzheimer's and Dementia, 2021. 17	0.4	0

Jianhua Wang

#	Article	IF	CITATIONS
19	Corneal epithelial thickness profile in dry-eye disease. Eye, 2020, 34, 915-922.	1.1	23
20	Reduced Retinal Microvascular Density Related to Activity Status and Serum Antibodies in Patients with Graves' Ophthalmopathy. Current Eye Research, 2020, 45, 576-584.	0.7	22
21	Unique changes in the retinal microvasculature reveal subclinical retinal impairment in patients with systemic lupus erythematosus. Microvascular Research, 2020, 129, 103957.	1.1	16
22	Characterization of retinal microvasculature and its relations to cognitive function in older people after circuit resistance training. Experimental Gerontology, 2020, 142, 111114.	1.2	6
23	Improved conjunctival microcirculation in diabetic retinopathy patients with MTHFR polymorphisms after Ocufolinâ,,¢ Administration. Microvascular Research, 2020, 132, 104066.	1.1	8
24	Characterization of the retinal vasculature in fundus photos using the PanOptic iExaminer system. Eye and Vision (London, England), 2020, 7, 46.	1.4	4
25	Wavelet Features of the Thickness Map of Retinal Ganglion Cell-Inner Plexiform Layer Best Discriminate Prior Optic Neuritis in Patients With Multiple Sclerosis. IEEE Access, 2020, 8, 221590-221598.	2.6	3
26	Reduced macular inner retinal thickness and microvascular density in the early stage of patients with dysthyroid optic neuropathy. Eye and Vision (London, England), 2020, 7, 16.	1.4	24
27	Conjunctival microvascular responses to anti-inflammatory treatment in patients with dry eye. Microvascular Research, 2020, 131, 104033.	1.1	4
28	Nutritional and medical food therapies for diabetic retinopathy. Eye and Vision (London, England), 2020, 7, 33.	1.4	41
29	Focal alteration of the intraretinal layers in neurodegenerative disorders. Annals of Eye Science, 2020, 5, 8-8.	1.1	3
30	Relationships among retinal/choroidal thickness, retinal microvascular network and visual field in high myopia. Acta Ophthalmologica, 2020, 98, e709-e714.	0.6	27
31	Visual Function and Disability Are Associated with Increased Retinal Volumetric Vessel Density in Patients with Multiple Sclerosis. American Journal of Ophthalmology, 2020, 213, 34-45.	1.7	28
32	Role of optical coherence tomography angiography in the characterization of vascular network patterns of ocular surface squamous neoplasia. Ocular Surface, 2020, 18, 926-935.	2.2	20
33	Deep Retinal Capillary Plexus Decreasing Correlated With the Outer Retinal Layer Alteration and Visual Acuity Impairment in Pathological Myopia. , 2020, 61, 45.		49
34	Conjunctival Vascular Adaptation Related to Ocular Comfort in Habitual Contact Lens Wearers. American Journal of Ophthalmology, 2020, 216, 99-109.	1.7	5
35	Associated risk factors in the early stage of diabetic retinopathy. Eye and Vision (London, England), 2019, 6, 23.	1.4	15
36	Improving diabetic and hypertensive retinopathy with a medical food containing L-methylfolate: a preliminary report. Eye and Vision (London, England), 2019, 6, 21.	1.4	11

#	Article	IF	CITATIONS
37	Photoreceptor Degeneration is Correlated With the Deterioration of Macular Retinal Sensitivity in High Myopia. , 2019, 60, 2800.		23
38	Focal Thickness Reduction of the Ganglion Cell-Inner Plexiform Layer Best Discriminates Prior Optic Neuritis in Patients With Multiple Sclerosis. , 2019, 60, 4257.		13
39	Deep perifoveal vessel density as an indicator of capillary loss in high myopia. Eye, 2019, 33, 1961-1968.	1.1	31
40	Zwitterion-functionalized dendrimer-entrapped gold nanoparticles for serum-enhanced gene delivery to inhibit cancer cell metastasis. Acta Biomaterialia, 2019, 99, 320-329.	4.1	71
41	Characterization of retinal microvasculature in acute non-arteritic anterior ischemic optic neuropathy using the retinal functional imager: a prospective case series. Eye and Vision (London,) Tj ETQq1 1	0.78 ft3 14	rgBѢ/Overloc
42	A review of functional slit lamp biomicroscopy. Eye and Vision (London, England), 2019, 6, 15.	1.4	15
43	Retinal Tissue Perfusion in Patients with Multiple Sclerosis. Current Eye Research, 2019, 44, 1091-1097.	0.7	8
44	Inter-visit measurement variability of conjunctival vasculature and circulation in habitual contact lens wearers and non-lens wearers. Eye and Vision (London, England), 2019, 6, 10.	1.4	4
45	Microcirculation in the conjunctiva and retina in healthy subjects. Eye and Vision (London, England), 2019, 6, 11.	1.4	5
46	Visual Function and Disability Are Associated With Focal Thickness Reduction of the Ganglion Cell-Inner Plexiform Layer in Patients With Multiple Sclerosis. , 2019, 60, 1213.		19
47	Quantitative analysis of conjunctival microvasculature imaged using optical coherence tomography angiography. Eye and Vision (London, England), 2019, 6, 5.	1.4	18
48	Age-Related Alterations in Retinal Tissue Perfusion and Volumetric Vessel Density. , 2019, 60, 685.		60
49	Loss of hypermethylated in cancer 1 (HIC1) promotes lung cancer progression. Cellular Signalling, 2019, 53, 162-169.	1.7	6
50	Functional slit lamp biomicroscopy metrics correlate with cardiovascular risk. Ocular Surface, 2019, 17, 64-69.	2.2	14
51	Posterior Condyle Offset and Maximum Knee Flexion Following a Cruciate Retaining Total Knee Arthroplasty. Journal of Knee Surgery, 2019, 32, 146-152.	0.9	3
52	Microvascular abnormalities in dry eye patients. Microvascular Research, 2018, 118, 155-161.	1.1	23
53	Axial elongation measured by long scan depth optical coherence tomography during pilocarpine-induced accommodation in intraocular lens-implanted eyes. Scientific Reports, 2018, 8, 1981.	1.6	5
54	A Mini Review of Clinical and Research Applications of the Retinal Function Imager. Current Eye Research, 2018, 43, 273-288.	0.7	24

2.2

32

#	ARTICLE	IF	CITATIONS
55	Evaluated Conjunctival Blood Flow Velocity in Daily Contact Lens Wearers. Eye and Contact Lens, 2018, 44, S238-S243.	0.8	17
56	Altered Macular Microvasculature in Mild Cognitive Impairment and Alzheimer Disease. Journal of Neuro-Ophthalmology, 2018, 38, 292-298.	0.4	141
57	Targeting CXCR7 improves the efficacy of breast cancer patients with tamoxifen therapy. Biochemical Pharmacology, 2018, 147, 128-140.	2.0	19
58	The inter-visit variability of retinal blood flow velocity measurements using retinal function imager (RFI). Eye and Vision (London, England), 2018, 5, 31.	1.4	4
59	Retinal nerve fiber layer (RNFL) integrity and its relations to retinal microvasculature and microcirculation in myopic eyes. Eye and Vision (London, England), 2018, 5, 25.	1.4	15
60	Retinal tissue hypoperfusion in patients with clinical Alzheimer's disease. Eye and Vision (London,) Tj ETQq0	0 0 rgBT /0 1.4	Overlock 10 T
61	Altered birefringence of peripapillary retinal nerve fiber layer in multiple sclerosis measured by polarization sensitive optical coherence tomography. Eye and Vision (London, England), 2018, 5, 14.	1.4	10
62	Visualization of Focal Thinning of the Ganglion Cell–Inner Plexiform Layer in Patients with Mild Cognitive Impairment and Alzheimer's Disease. Journal of Alzheimer's Disease, 2018, 64, 1261-1273.	1.2	45
63	Characteristics of Retinal Structural and Microvascular Alterations in Early Type 2 Diabetic Patients. , 2018, 59, 2110.		38
64	Retinal Microvascular Impairment in the Early Stages of Parkinson's Disease. , 2018, 59, 4115.		86
65	Factors Affecting Microvascular Responses in the Bulbar Conjunctiva in Habitual Contact Lens Wearers. , 2018, 59, 4108.		16
66	Optical coherence tomography for ocular surface and corneal diseases: a review. Eye and Vision (London, England), 2018, 5, 13.	1.4	59
67	Long scan depth optical coherence tomography on imaging accommodation: impact of enhanced axial resolution, signal-to-noise ratio and speed. Eye and Vision (London, England), 2018, 5, 16.	1.4	5

68	Impaired retinal microcirculation in patients with Alzheimer's disease. PLoS ONE, 2018, 13, e0192154.	1.1	41	
69	Altered Bulbar Conjunctival Microcirculation in Response to Contact Lens Wear. Eye and Contact Lens, 2017, 43, 95-99.	0.8	20	

Bulbar conjunctival microvascular responses in dry eye. Ocular Surface, 2017, 15, 193-201.

71	InÂVivo Characteristics of Corneal Endothelium/Descemet Membrane Complex for the Diagnosis of Corneal Graft Rejection. American Journal of Ophthalmology, 2017, 178, 27-37.	1.7	27
72	Role of high resolution optical coherence tomography in diagnosing ocular surface squamous neoplasia with coexisting ocular surface diseases. Ocular Surface, 2017, 15, 688-695.	2.2	54

5

#	Article	IF	CITATIONS
73	Characteristic of entire corneal topography and tomography for the detection of sub-clinical keratoconus with Zernike polynomials using Pentacam. Scientific Reports, 2017, 7, 16486.	1.6	34
74	Retinal Microvascular Network and Microcirculation Assessments in High Myopia. American Journal of Ophthalmology, 2017, 174, 56-67.	1.7	162
75	Age-Related Alterations in the Retinal Microvasculature, Microcirculation, and Microstructure. , 2017, 58, 3804.		118
76	Characterization of Soft Contact Lens Fitting Using Ultra-Long Scan Depth Optical Coherence Tomography. Journal of Ophthalmology, 2017, 2017, 1-13.	0.6	4
77	Comparison of Retinal Microvessel Blood Flow Velocities Acquired with Two Different Fields of View. Journal of Ophthalmology, 2017, 2017, 1-7.	0.6	4
78	The Relationship Between High-Order Aberration and Anterior Ocular Biometry During Accommodation in Young Healthy Adults. , 2017, 58, 5628.		11
79	MiR-206 suppresses epithelial mesenchymal transition by targeting TGF-Î ² signaling in estrogen receptor positive breast cancer cells. Oncotarget, 2016, 7, 24537-24548.	0.8	66
80	Retinal Microvasculature Alteration in High Myopia. , 2016, 57, 6020.		125
81	Vessel Sampling and Blood Flow Velocity Distribution With Vessel Diameter for Characterizing the Human Bulbar Conjunctival Microvasculature. Eye and Contact Lens, 2016, 42, 135-140.	0.8	32
82	Value of corneal epithelial and Bowman's layer vertical thickness profiles generated by UHR-OCT for sub-clinical keratoconus diagnosis. Scientific Reports, 2016, 6, 31550.	1.6	26
83	Lid Wiper Microvascular Responses as an Indicator of Contact Lens Discomfort. American Journal of Ophthalmology, 2016, 170, 197-205.	1.7	15
84	InÂVivo Characterization of Retinal Microvascular Network in Multiple Sclerosis. Ophthalmology, 2016, 123, 437-438.	2.5	24
85	Impaired retinal microcirculation in multiple sclerosis. Multiple Sclerosis Journal, 2016, 22, 1812-1820.	1.4	46
86	Wavefront Derived Refraction and Full Eye Biometry in Pseudophakic Eyes. PLoS ONE, 2016, 11, e0152293.	1.1	6
87	Targeted delivery of doxorubicin by lactobionic acid-modified laponite to hepatocarcinoma cells. Journal of Controlled Release, 2015, 213, e34.	4.8	5
88	In vivo quantification of cochlin in glaucomatous DBA/2J mice using optical coherence tomography. Scientific Reports, 2015, 5, 11092.	1.6	7
89	Slitlamp Photography and Videography With High Magnifications. Eye and Contact Lens, 2015, 41, 391-397.	0.8	9

#	Article	IF	CITATIONS
91	Author Response: Human Accommodative Ciliary Muscle Configuration Changes Are Consistent With Schachar's Mechanism of Accommodation. , 2015, 56, 6076.		3
92	The Impact of Flap Creation Methods for Sub-Bowman's Keratomileusis (SBK) on the Central Thickness of Bowman's Layer. PLoS ONE, 2015, 10, e0124996.	1.1	3
93	Neurostimulation of the Lacrimal Nerve for Enhanced Tear Production. Ophthalmic Plastic and Reconstructive Surgery, 2015, 31, 145-151.	0.4	21
94	Targeted doxorubicin delivery to hepatocarcinoma cells by lactobionic acid-modified laponite nanodisks. New Journal of Chemistry, 2015, 39, 2847-2855.	1.4	56
95	Measurement variability of the bulbar conjunctival microvasculature in healthy subjects using functional slit lamp biomicroscopy (FSLB). Microvascular Research, 2015, 101, 15-19.	1.1	30
96	Ultra high resolution optical coherence tomography in Boston type I keratoprosthesis. Journal of Ophthalmic and Vision Research, 2015, 10, 26.	0.7	17
97	Vertical and Horizontal Corneal Epithelial Thickness Profile Using Ultra-High Resolution and Long Scan Depth Optical Coherence Tomography. PLoS ONE, 2014, 9, e97962.	1.1	21
98	Whole Eye Axial Biometry During Accommodation Using Ultra-long Scan Depth Optical Coherence Tomography. American Journal of Ophthalmology, 2014, 157, 1064-1069.e2.	1.7	39
99	Axial Biometry of the Entire Eye Using Ultra-Long Scan Depth Optical Coherence Tomography. American Journal of Ophthalmology, 2014, 157, 412-420.e2.	1.7	14
100	The Use of Bowman's Layer Vertical Topographic Thickness Map in the Diagnosis of Keratoconus. Ophthalmology, 2014, 121, 988-993.	2.5	57
101	Functional slit lamp biomicroscopy for imaging bulbar conjunctival microvasculature in contact lens wearers. Microvascular Research, 2014, 92, 62-71.	1.1	54
102	Ultra High-Resolution Anterior Segment Optical Coherence Tomography in the Diagnosis and Management of Ocular Surface Squamous Neoplasia. Ocular Surface, 2014, 12, 46-58.	2.2	134
103	Automated segmentation and fractal analysis of high-resolution non-invasive capillary perfusion maps of the human retina. Microvascular Research, 2013, 89, 172-175.	1.1	36
104	Diagnosis of Ocular Surface Lesions Using Ultra–High-Resolution Optical Coherence Tomography. Ophthalmology, 2013, 120, 883-891.	2.5	86
105	Human conjunctival microvasculature assessed with a retinal function imager (RFI). Microvascular Research, 2013, 85, 134-137.	1.1	22
106	Simultaneous real-time imaging of the ocular anterior segment including the ciliary muscle during accommodation. Biomedical Optics Express, 2013, 4, 466.	1.5	36
107	Versatile optical coherence tomography for imaging the human eye. Biomedical Optics Express, 2013, 4, 1031.	1.5	32
108	The TFOS International Workshop on Contact Lens Discomfort: Report of the Contact Lens Interactions With the Tear Film Subcommittee. , 2013, 54, TFOS123.		167

#	Article	IF	CITATIONS
109	Phacoemulsification Induced Transient Swelling of Corneal Descemet's Endothelium Complex Imaged with Ultra-High Resolution Optical Coherence Tomography. PLoS ONE, 2013, 8, e80986.	1.1	26
110	Repeated Measurements of the Anterior Segment During Accommodation Using Long Scan Depth Optical Coherence Tomography. Eye and Contact Lens, 2012, 38, 102-108.	0.8	33
111	Daytime Variations of Tear Osmolarity and Tear Meniscus Volume. Eye and Contact Lens, 2012, 38, 282-287.	0.8	45
112	Visualization of the Precorneal Tear Film Using Ultrahigh Resolution Optical Coherence Tomography in Dry Eye. Eye and Contact Lens, 2012, 38, 240-244.	0.8	14
113	Automatic Segmentation of the Central Epithelium Imaged With Three Optical Coherence Tomography Devices. Eye and Contact Lens, 2012, 38, 150-157.	0.8	20
114	Clinical Significance of Tear Menisci in Dry Eye. Eye and Contact Lens, 2012, 38, 183-187.	0.8	28
115	Vertical and Horizontal Corneal Epithelial Thickness Profiles Determined by Ultrahigh Resolution Optical Coherence Tomography. Cornea, 2012, 31, 1036-1043.	0.9	38
116	Effect of Punctal Occlusion on Tear Menisci in Symptomatic Contact Lens Wearers. Cornea, 2012, 31, 1014-1022.	0.9	11
117	Anterior Segment Biometry during Accommodation Imaged with Ultralong Scan Depth Optical Coherence Tomography. Ophthalmology, 2012, 119, 2479-2485.	2.5	57
118	Ultra-High Resolution Optical Coherence Tomography for Differentiation of Ocular Surface Squamous Neoplasia and Pterygia. Ophthalmology, 2012, 119, 481-486.	2.5	135
119	Micrometer-Scale Contact Lens Movements Imaged by Ultrahigh-resolution Optical Coherence Tomography. American Journal of Ophthalmology, 2012, 153, 275-283.e1.	1.7	14
120	Synthesis of glycoconjugated poly(amindoamine) dendrimers for targeting human liver cancer cells. RSC Advances, 2012, 2, 99-102.	1.7	37
121	Ultra-high resolution optical coherence tomography for monitoring tear meniscus volume in dry eye after topical cyclosporine treatment. Clinical Ophthalmology, 2012, 6, 933.	0.9	18
122	Cochlin, Intraocular Pressure Regulation and Mechanosensing. PLoS ONE, 2012, 7, e34309.	1.1	36
123	Slit-Lamp–Adapted Ultra-High Resolution OCT for Imaging the Posterior Segment of the Eye. Ophthalmic Surgery Lasers and Imaging Retina, 2012, 43, 76-81.	0.4	10
124	In Vivo Morphologic Characteristics of Salzmann Nodular Degeneration With Ultra-High-Resolution Optical Coherence Tomography. American Journal of Ophthalmology, 2011, 151, 248-256.e2.	1.7	28
125	Diagnosis and Management of Conjunctival and Corneal Intraepithelial Neoplasia Using Ultra High-Resolution Optical Coherence Tomography. Ophthalmology, 2011, 118, 1531-1537.	2.5	90
126	Tear Menisci and Ocular Discomfort during Daily Contact Lens Wear in Symptomatic Wearers. , 2011, 52, 2175.		47

Jianhua Wang

#	Article	IF	CITATIONS
127	Topographic Thickness of Bowman's Layer Determined by Ultra-High Resolution Spectral Domain–Optical Coherence Tomography. , 2011, 52, 3901.		78
128	The Watery Eye. Current Allergy and Asthma Reports, 2011, 11, 192-196.	2.4	2
129	Evaluation of a Transgenic Mouse Model of Multiple Sclerosis with Noninvasive Methods. , 2011, 52, 2405.		22
130	Characterization of Soft Contact Lens Edge Fitting Using Ultra-High Resolution and Ultra-Long Scan Depth Optical Coherence Tomography. , 2011, 52, 4091.		53
131	Broadband superluminescent diode–based ultrahigh resolution optical coherence tomography for ophthalmic imaging. Journal of Biomedical Optics, 2011, 16, 126006.	1.4	27
132	Age-Related Changes in Tear Menisci Imaged by Optical Coherence Tomography. Optometry and Vision Science, 2011, 88, 1214-1219.	0.6	28
133	Tear Menisci after Overnight Contact Lens Wear. Optometry and Vision Science, 2011, 88, 1433-1438.	0.6	7
134	Ultra-High Resolution Optical Coherence Tomography for Imaging the Anterior Segment of the Eye. Ophthalmic Surgery Lasers and Imaging Retina, 2011, 42, S15-27.	0.4	66
135	Upper and Lower Tear Menisci After Laser In Situ Keratomileusis. Eye and Contact Lens, 2010, 36, 81-85.	0.8	18
136	Entire Contact Lens Imaged In Vivo and In Vitro With Spectral Domain Optical Coherence Tomography. Eye and Contact Lens, 2010, 36, 73-76.	0.8	33
137	Detection of Magnetic Particles in Live DBA/2J Mouse Eyes Using Magnetomotive Optical Coherence Tomography. Eye and Contact Lens, 2010, 36, 346-351.	0.8	11
138	Upper Punctal Occlusion versus Lower Punctal Occlusion in Dry Eye. , 2010, 51, 5571.		28
139	Tear Meniscus Volume in Dry Eye after Punctal Occlusion. , 2010, 51, 1965.		34
140	Ultrahigh-Resolution Measurement by Optical Coherence Tomography of Dynamic Tear Film Changes on Contact Lenses. , 2010, 51, 1988.		81
141	Use of Ultra-High-Resolution Optical Coherence Tomography to Detect In Vivo Characteristics of Descemet's Membrane in Fuchs' Dystrophy. Ophthalmology, 2010, 117, 1220-1227.	2.5	104
142	Reduced Tear Meniscus Dynamics in Dry Eye Patients With Aqueous Tear Deficiency. American Journal of Ophthalmology, 2010, 149, 932-938.e1.	1.7	33
143	Disruption of tear film and blink dynamics. , 2010, , 123-130.		1
144	In Vivo Structural Characteristics of the Femtosecond LASIK-Induced Opaque Bubble Layers with Ultrahigh-Resolution SD-OCT. Ophthalmic Surgery Lasers and Imaging Retina, 2010, 41, S109-13.	0.4	26

#	Article	IF	CITATIONS
145	SD-OCT with Prolonged Scan Depth for Imaging the Anterior Segment of the Eye. Ophthalmic Surgery Lasers and Imaging Retina, 2010, 41, S65-9.	0.4	40
146	Lower Volumes of Tear Menisci in Contact Lens Wearers with Dry Eye Symptoms. , 2009, 50, 3159.		66
147	Upper and Lower Tear Menisci in the Diagnosis of Dry Eye. , 2009, 50, 2722.		136
148	In Situ Visualization of Tears on Contact Lens Using Ultra High Resolution Optical Coherence Tomography. Eye and Contact Lens, 2009, 35, 44-49.	0.8	59
149	Diurnal Variation of Upper and Lower Tear Menisci. American Journal of Ophthalmology, 2008, 145, 801-806.e2.	1.7	73
150	Correlations Among Upper and Lower Tear Menisci, Noninvasive Tear Break-up Time, and the Schirmer Test. American Journal of Ophthalmology, 2008, 145, 795-800.e1.	1.7	110
151	Effect of Blinking on Tear Volume After Instillation of Midviscosity Artificial Tears. American Journal of Ophthalmology, 2008, 146, 920-924.	1.7	41
152	Dynamic Distribution of Artificial Tears on the Ocular Surface. JAMA Ophthalmology, 2008, 126, 619.	2.6	47
153	Diurnal Variation of Ocular Hysteresis, Corneal Thickness, and Intraocular Pressure. Optometry and Vision Science, 2008, 85, 1185-1192.	0.6	47
154	CRF-Based Segmentation of Human Tear Meniscus Obtained with Optical Coherence Tomography. , 2007, , .		1
155	Effect of Blinking on Tear Dynamics. , 2007, 48, 3032.		130
156	Relationships between Central Tear Film Thickness and Tear Menisci of the Upper and Lower Eyelids. Investigative Ophthalmology and Visual Science, 2006, 47, 4349-4355.	3.3	127
157	Repeated Measurements of Dynamic Tear Distribution on the Ocular Surface after Instillation of Artificial Tears. , 2006, 47, 3325.		110
158	Noncontact Measurements of Central Corneal Epithelial and Flap Thickness after Laser In Situ Keratomileusis. , 2004, 45, 1812.		94
159	Precorneal and Pre- and Postlens Tear Film Thickness Measured Indirectly with Optical Coherence Tomography. , 2003, 44, 2524.		186
160	Topographical Thickness of the Epithelium and Total Cornea after Overnight Wear of Reverse-Geometry Rigid Contact Lenses for Myopia Reduction. , 2003, 44, 4742.		113
161	The measurement of corneal epithelial thickness in response to hypoxia using optical coherence tomography11Proprietary interests: The authors have no proprietary interest in any materials or methods described within this article American Journal of Ophthalmology, 2002, 133, 315-319.	1.7	100
162	Relation between optical coherence tomography and optical pachymetry measurements of corneal swelling induced by hypoxia. American Journal of Ophthalmology, 2002, 134, 93-98.	1.7	59

#	Article	IF	CITATIONS
163	TOPOGRAPHICAL THICKNESS OF THE EPITHELIUM AND TOTAL CORNEA AFTER HYDROGEL AND PMMA CONTACT LENS WEAR WITH EYE CLOSURE Optometry and Vision Science, 2001, 78, 303.	0.6	1
164	(CL-115)THE MEASUREMENT OF CORNEAL EPITHELIAL THICKNESS USING OPTICAL COHERENCE TOMOGRAPHY IN RESPONSE TO HYPOXIA INDUCED BY SOFT CONTACT LENS AND EYE CLOSURE. Optometry and Vision Science, 2000, 77, 170.	0.6	2
165	Vectorcardiographic Evaluation of Myocardial Infarct Size. Japanese Circulation Journal, 1998, 62, 473-478.	1.0	5
166	Improved Retinal Microcirculation in Mild Diabetic Retinopathy Patients Carrying MTHFR Polymorphisms Who Received the Medical Food, Ocufolin®. Clinical Ophthalmology, 0, Volume 16, 1497-1504.	0.9	3